Cooperative Positioning of Wireless Networks in Complex Propagation Environments

Peiyue Jiang, Xiaobo Gu, and Haibo Zhou, *Senior Member, IEEE*

***Abstract*— Cooperative positioning in wireless networks has attracted great attention in recent years, as many applications require the exact location of all member nodes. The pairwise distance between the member nodes is conventionally constructed as an Euclidean Distance Matrix (EDM) for subsequent location estimation. In this paper, we address the problem of cooperative positioning in complex propagation environments, which results in an incomplete EDM. We proposed an improved EDM recovery algorithm based on low tank matrix completion (LRMC), which makes use of the sensor correlation by Laplacian and trace minimization. In addition, we derive a semi-definite relaxation estimator to localize the unknown sensors. Simulations are conducted to evaluate the performance of the proposed algorithm and the results show that the proposed method outperforms existing ones in both matrix completion and positioning accuracy.**

***Index Terms*— Cooperative positioning, graph Laplacian, low rank matrix completion, manifold learning, semi-definite programming.**

I. Introduction

ESTIMATING the positions of the member nodes in a wireless sensor network (WSN) is a key requirement in numerous applications. Distance-based positioning arises in the last decades since the global navigation satellite system (GNSS) signals are unavailable in certain harsh environments. In this case, constructing an ad hoc network for an inaccessible network using wireless signals is a feasible solution. Various methods can be used to measure the relative distance between members, for example, time of arrival (TOA), time difference of arrival (TDOA) and received signal strength (RSS). For TOA and TDOA, the exchanged timing stamps are used to measure distance, while for RSS, the relative distance is measured by signal fading. These techniques depend on the visibility of the communication link, namely, the signals are required to be transmitted without interference or occlusion.

Furthermore, a variety of distance-based algorithms can be implemented to estimate the locations of the member nodes, such as multidimensional scaling (MDS) [1] and multilateration [2]. When performing the MDS-based positioning, the ranging measurements are required to be collected to construct an Euclidean distance matrix (EDM). That is to say, the MDS-based algorithms require a complete EDM as the input and then output the relative location of nodes. A step further, the absolute positioning can be completed by applying a rotation and translation transformation between the relative coordinates and absolute coordinates [1], [3]. In the case of multilateration, the three dimensional position of the unknown node is estimated by the intersection of four circles whose centres are known in advance and the measured relative distances are treated as radii. Recently, a number of low-complexity and high accuracy positioning algorithms based on incomplete ranging information have been proposed [4], [5], [6], [7]. However, it should be noted that the increasing ranging measurements can improve the positioning accuracy from the perspective of statistical signal processing. In a word, the ranging measurement recovery is a feasible way to improve the positioning accuracy.

In practice, the communication links between the members can not keep visible all the time owing to energy saving, limited communication radius and electromagnetic interference, which results in an incomplete EDM [8]. To overcome this problem, a number of algorithms have been proposed to estimate these unknown distances. The relative kinematics model is implemented to perform cooperative positioning based on incomplete EDM. A relative positioning model can be utilized by using the velocity measurements [9], [10], [11]. In [9], the authors propose a discrete time state space model which consists of position and velocity, and an extended Kalman filter (EKF) estimator is presented. These methods, however, require Doppler measurements, which are difficult to measure under certain circumstances. Meanwhile, it also increases the overall cost and energy consumption. The semi-definite programming (SDP) method is proposed to perform location estimation without velocity measurements, and it improves the estimation accuracy by using the maximum and/or minimum communication radius as the prior information [12], [13], [14]. However, it has been shown that these algorithms based on the prior information are not able to estimate the invisible pairwise distances, but can only be used to perform positioning. Recovering the incomplete matrix from partial observations has led to a fast emerging field of research, which has been refereed as compressed sensing [15], [16], [17], cooperative filtering [18] and low rank matrix completion (LRMC) [8], [19]. Extensive solutions have been proposed in recent years for estimating the inaccessible pairwise distances based on LRMC. The existing works reveal that the EDM has the property of low rank,

Manuscript received 3 November 2023; revised 20 March 2024; accepted 7 May 2024. Date of publication 14 June 2024; date of current version 18 September 2024. This work was supported in part by the National Natural Science Foundation of China under Grant 62101138 and Grant 62271244, in part by Guangdong Natural Science Foundation under Grant 2022A1515012573, and in part by the Natural Science Fund for Distinguished Young Scholars of Jiangsu Province under Grant BK20220067. *(Corresponding authors: Xiaobo Gu; Haibo Zhou.)*

Peiyue Jiang and Xiaobo Gu are with the School of Integrated Circuits, Guangdong University of Technology, Guangzhou 510006, China (e-mail: xiaobo.gu@gdut.edu.cn).

Haibo Zhou is with the School of Electronic Science and Engineering, Nanjing University, Nanjing 210008, China (e-mail: h53zhou@uwaterloo.ca).

Color versions of one or more figures in this article are available at https://doi.org/10.1109/JSAC.2024.3414589.

Digital Object Identifier 10.1109/JSAC.2024.3414589

based on which, a number of algorithms are implemented to recover the EDM [8], [20], [21]. After that, the recovered EDM can be used for cooperative positioning. However, all these propositions are based on the classical LRMC, in which matrix elements are assumed to be unorganized, so that the correlation between the member nodes is not taken into account.

In this paper, we address the problem of EDM completion of a partially connected WSN. The network members measure the pairwise distances by using the ranging techniques such as TOA and RSS. In addition, some of the member nodes are set as anchors to provide a reference coordinate system for the other sensor nodes. The anchor positions and maximum communication radius of the member nodes are considered as the prior knowledge to estimate the locations of the sensor nodes. We propose a novel method incorporating the correlation among the EDM elements, which improves the performance of EDM recovery.

A. Applications and Related Works

The motivation for this work is to achieve cooperative positioning based on incomplete EDM, namely, only partial ranging measurements can be collected owing to complex propagation environments. By investigating the relationship between the performance of distance-based positioning techniques and the completeness of EDM, we aim to solve the problem of EDM recovery to improve the performance of cooperative positioning, which can be widely applied in wireless networks, including deep space exploration, underwater WSN, environmental monitoring, internet of vehicles, space-air-ground integrated network and unmanned aerial vehicle swarms.

Similar to other matrix completion applications, such as traffic sensing [22], [23] and recommendation systems [24], [25], [26], the problem presented in this paper can be considered as a rank minimization problem of partial ranging measurements. Since this problem is non-deterministic polynomial (NP)-hard and non-convex [27], researchers initially exploit the heuristically search to solve this problem [28], [29]. In principle, the solution will lead to the problem of local optimum. Candès and Tao propose the approximated rank minimization algorithms by solving the problem of minimum nuclear norm [30], [31] and consequently arise a series of works. The classical singular value thresholding (SVT) approximates the matrix with minimum nuclear norm among all matrices obeying a set of convex constraints [32]. Numerous related existing algorithms also utilize this approximation to recover the incomplete matrix [33], [34], [35], [36]. A step further, if the matrix is a positive semi-definite (PSD) matrix, the rank minimization process can be regarded as a trace minimization problem [27]. Considering that the EDM is not a PSD matrix, a lemma for the non-PSD matrix recovery by constructing a PSD matrix is proposed in [27]. A survey on matrix completion from a signal processing perspective is presented in [33]. However, a well known drawback of trace minimization is that its performance would be significantly decreased when entries of the matrix are sampled non-uniformly [37]. Cai et al. [38] prove that the max norm is minimax rate-optimal under non-uniform sampling, and thus arises the algorithm proposed in [39].

However, all these propositions are based on the classical LRMC, where the elements of matrix are assumed to be unorganized, so that the correlation between these elements are neglected. A number of algorithms are used to analyze the relationship among agents in WSNs. In [19], the authors applied the Hodges-Lehmann (HL) test to characterize the correlation among the member nodes when positioning the unknown sensors based on SVT. However, the correlation tests are implemented for anchor selection rather than matrix recovery. In [18], an algorithm based on the nuclear norm approximation is proposed, which takes the correlations into account to recover the movie or product recommendation matrix via user graphs. The label information of users and movies are used for constructing the graphs, the greater the number of labels that a user and a movie have the same, the greater the edge weight. Additionally, the Laplacian operation can be adopted to construct a low-dimensional manifold from a high-dimensional vector, which is capable of preserving the distribution characteristics of the data and smoothing the solution in manifold, [40], [41]. In a word, to the best of our knowledge, making use of the correlation between the nodes via graphs to solve the problem of LRMC-based positioning is novel.

B. Contributions and Outline

In order to achieve cooperative positioning in complex propagation environments, we propose a LRMC method to recover the EDM. The contributions of this paper can be briefly summarized as follows:

- We propose a sensor correlation representation and quantification framework in Section III-A to perform cooperative positioning. A weighted undirected graph is used to represent the sensor correlation, and the weight matrix is determined by the relative distance between the members.
- In light of that Laplacian provides a convex objective function and a solution smooth on graph, a novel SEDM completion algorithm based on SDP is proposed (in Section III-B, (36)) for partially connected WSNs, where we incorporate the low rank property and sensor correlation into optimization objective to recover the incomplete matrix.
- Based on the recovered distance matrix, we develop a semi-definite relaxation estimator (39) in Section III-C for subsequent cooperative positioning, which is able to estimate the location of the unknown sensors.

The rest of the paper is structured as follows. In Section II, we model the EDM completion problem as a LRMC problem based on two ranging techniques, and then present a SDP positioning algorithm. In Section III, the novel sensor graphs and correlation assisted matrix completion algorithm is introduced to solve the problem of locating unknown sensors. The simulations are presented and discussed in Section IV. The conclusions are provided in Section V.

C. Notations

$(\cdot)^T$ denotes the matrix transpose operator. $\mathbf{I}_N$ represents a N-dimensional identity matrix, $\mathbf{1}_N = [1, 1, \cdots, 1]^T$ and $\mathbf{0}_N = [0, 0, \cdots, 0]^T$. $\odot$ stands for the Hadamard product operator. $[\mathbf{A}]_{ij}$ represents the i^{th} row jth column element of matrix $\mathbf{A}$, $[\mathbf{A}]_{.i}$ represents the i^{th} column of matrix $\mathbf{A}$ and $[\mathbf{A}]_{i.}$

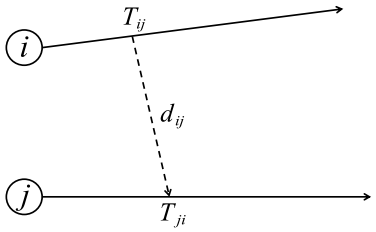

Fig. 1. The schematic diagram of TOA ranging. Nodes are capable of communicating with each other, the timestamp transmission direction is not mandatory. Take this schematic diagram as an example, node i represents the timestamp transmitter and node j represents the receiver, the timestamp transmission direction is from i to j. Therefore, $T_{ij} < T_{ji}$, namely, $(T_{ji} - T_{ij})$ is positive.

represents the i^{th} row of the matrix $\mathbf{A}$. $\hat{\cdot}$ denotes the estimation and $\widetilde{\cdot}$ denotes the measurement. Let $\|\cdot\|_*$,$\|\cdot\|_F$, $\|\cdot\|_2$ and $\|\cdot\|_D$ denote the nuclear norm (i.e., the sum of singular values), the Frobenius norm, ℓ_2 norm and graph Dirichlet semi-norm, respectively. And $\mathrm{Tr}(\mathbf{A})$ stands for the trace of matrix $\mathbf{A}$. $\succeq$ stands for the matrix inequality. Let $|\mathcal{A}|$ denote the number of elements in set $\mathcal{A}$.

II. System Model

A. Ranging Model

We consider a WSN of N node with positions $\mathbf{X} = \left[\boldsymbol{x}_1, \cdots, \boldsymbol{x}_N\right] \in \mathbb{R}^{D\times N}$ in a D-dimension ($D = 2$ or 3) space. The positions of N_a nodes are known in advance, which we referred to as anchor nodes. As for the remaining $N_u(= N - N_a)$ sensors, their positions are unknown and required to be estimated. Without loss of generality, we assume that the 1^{st} to N_a^{th} nodes are anchor nodes, while the $(N_a+1)^{th}$ to N^{th} nodes are unknown sensor nodes. Thus, $\mathbf{X}$ can be divided into $\mathbf{A} = \left[\boldsymbol{a}_1, \cdots, \boldsymbol{a}_N\right] \in \mathbb{R}^{D\times N_a}$ and $\mathbf{U} = \left[\boldsymbol{u}_1, \cdots, \boldsymbol{u}_N\right] \in \mathbb{R}^{D\times N_u}$, which represent the position of anchor nodes and sensor nodes, respectively, expressed as

$$\begin{aligned}\mathbf{X} &\triangleq \begin{bmatrix}\boldsymbol{a}_1 & \cdots & \boldsymbol{a}_{N_a} & \boldsymbol{u}_1 & \cdots & \boldsymbol{u}_{N_u}\end{bmatrix} \\ &= \begin{bmatrix}\mathbf{A} & \mathbf{U}\end{bmatrix}\end{aligned} \tag{1}$$

The relative distances between nodes can be measured by various ranging techniques. In this paper, we discuss the TOA and RSS ranging techniques for the sake of illustration. We will introduce these two types of ranging techniques and present simulation results separately in the two different scenarios.

1) TOA Ranging: As shown in Fig. 1, node i sends a timing stamp which records the transmitting time tag T_{ij} and the reception time tag T_{ji} is recorded at node j once the timing stamp has been received. The relative distance between node i and node j can be given by

$$\begin{aligned}d_{ij} &= c(T_{ji} - T_{ij}) \\ &= \|\boldsymbol{x}_i - \boldsymbol{x}_j\|_2,\end{aligned} \tag{2}$$

where c is the speed of the electromagnetic wave in the medium whose value depends on the environment. $i, j \in \{1, 2, \cdots, N\}$ denote the indices of sensors. The ranging measurement noise η_{ij} can be considered as Gaussian noise with zeros mean and variance σ^2, namely, $\eta_{ij} \sim \mathcal{N}(0, \sigma^2)$ [8], [42]. Then the measured relative distance can be expressed as

$$\widetilde{d}_{ij} = d_{ij} + \eta_{ij}. \tag{3}$$

We assume that the clocks have been perfectly synchronized, since the synchronization problem of TOA-based ranging has been discussed in a variety of existing literature [1], [2], [43], [44], and is beyond the scope of this paper.

2) RSS Ranging: The processing of RSS ranging can be summarized as follows, node i transmits a wireless signal to node j, then node j receives a P_{ij} mW signal if this signal could be acquired. P_{ij} is modeled as the log-normal shadowing path-loss model in this process:

$$P_{ij} = P_0 - 10n_p \log_{10}(d_{ij}/d_0), \tag{4}$$

where n_p is the path loss exponent, d_0 represents the reference distance which is related to the received power P_0. The RSS measurements are assumed to be plagued by the additive Gaussian white noise [20], [21] given by

$$\begin{aligned}\widetilde{P}_{ij} &= P_{ij} + q_{ij}, \\ q_{ij} &\sim \mathcal{N}(0, \sigma_r^2).\end{aligned} \tag{5}$$

According to (4), the pairwise distance can be estimated by the strength of $\widetilde{P}_{ij}$:

$$\widetilde{d}_{ij} = d_0 10^{(P_0 - \widetilde{P}_{ij})/(10n_p)}. \tag{6}$$

Since the RSS is inversely proportional to the pairwise distance, the RSS-based ranging is only valid within a certain radius.

3) Maximum Likelihood Estimator: Based on limited distance information, the maximum likelihood estimator (MLE) for estimating the positions can be expressed by

$$\min \sum_{(i,j)\in\mathcal{I}} \left\| \|\boldsymbol{x}_i - \boldsymbol{x}_j\|_2 - \widetilde{d}_{ij} \right\|_2^2, \tag{7}$$

where $\mathcal{I}$ is the set that consists of the communicated pair indices, and more details about $\mathcal{I}$ will be discussed in section II-C. However, (7) is non-convex [10, page 1] which is difficult to solve and cannot guarantee global optimality. Therefore, we define the squared distance $s_{ij} \triangleq d_{ij}^2$ which can be helpful to modify (7) as a SDP problem (in Section II-D).

B. Rank of Distance Matrices

In this section, we briefly prove that the squared Euclidean distance matrix (SEDM) and its sub-matrices are low rank matrix.

Referring to EDM $\mathbf{D}$ which lets $[\mathbf{D}]_{ij} = d_{ij}$, one can rearrange the distance information as a SEDM, expressed as

$$\mathbf{S} = \begin{bmatrix} 0 & s_{12} & \cdots & s_{1N} \\ s_{21} & 0 & \cdots & s_{2N} \\ \vdots & \vdots & \ddots & \vdots \\ s_{N1} & \cdots & \cdots & 0 \end{bmatrix}. \tag{8}$$

According to (1), $\mathbf{S}$ can be rewritten as

$$\mathbf{S} = \left[\begin{array}{c|c} \mathbf{S}_{aa} & \mathbf{S}_{au} \\ \hline \mathbf{S}_{au}^T & \mathbf{S}_{uu} \end{array}\right], \tag{9}$$

where $\mathbf{S}_{aa} \in \mathbb{R}^{N_a \times N_a}$ is the sub-matrix denoting the pairwise distance between all anchors, namely, the SEDM of anchors. $\mathbf{S}_{au} \in \mathbb{R}^{N_a \times N_u}$ is the sub-matrix denoting the pairwise distances between anchors and unknown sensors. $\mathbf{S}_{uu} \in \mathbb{R}^{N_u \times N_u}$ denotes the sub SEDM of unknown sensors. In practice, both $\mathbf{S}_{au}$ and $\mathbf{S}_{uu}$ are contaminated with noise. We assume that all the relative distances between anchors are accurately measured in advance, namely $\mathbf{S}_{aa} = \widetilde{\mathbf{S}}_{aa}$.

Observing (2), $\mathbf{S}$ can be rewritten as:

$$\mathbf{S} = \underline{\mathbf{X}}\mathbf{1}_N^T - 2\mathbf{X}^T\mathbf{X} + \mathbf{1}_N\underline{\mathbf{X}}^T, \tag{10}$$

where

$$\underline{\mathbf{X}} = \begin{bmatrix} \boldsymbol{x}_1^T\boldsymbol{x}_1 & \boldsymbol{x}_2^T\boldsymbol{x}_2 & \cdots & \boldsymbol{x}_N^T\boldsymbol{x}_N \end{bmatrix}^T \in \mathbb{R}^{N\times 1}. \tag{11}$$

It should be noted that $\underline{\mathbf{X}}$ is a rank-1 matrix, and thus $\text{rank}(\underline{\mathbf{X}}\mathbf{1}_N^T) = \text{rank}(\mathbf{1}_N\underline{\mathbf{X}}^T) \leq \min\{\text{rank}(\underline{\mathbf{X}}), \text{rank}(\mathbf{1}_N^T)\} = 1$. On the other hand, D-dimensional coordinate matrix $\mathbf{X}$ is a rank-D matrix if all nodes are not co-line. Therefore, we can infer that $\text{rank}(2\mathbf{X}\mathbf{X}^T) \leq \min\{\text{rank}(\mathbf{X}), \text{rank}(\mathbf{X}^T)\} = \text{rank}(\mathbf{X}) = D$. Accordingly, the rank of $\mathbf{S}$ is at most $D+2$, which implies that $\mathbf{S}$ is a low rank matrix when $N > D+2$. Similarly, as $\mathbf{S}_{aa}$ and $\mathbf{S}_{uu}$ are also SEDMs, they can also be proved to be low rank matrices.

A step further, we analyze the rank of sub-matrices $\mathbf{S}_{au}$ for the following matrix completion based on graph algorithms. $\mathbf{S}_{au}$ can be represented by

$$\mathbf{S}_{au} = \underline{\mathbf{A}} - 2\mathbf{A}^T\mathbf{U} + \underline{\mathbf{U}}, \tag{12}$$

where

$$\underline{\mathbf{A}} = \begin{bmatrix} \|\boldsymbol{a}_1\|_2^2 \\ \|\boldsymbol{a}_2\|_2^2 \\ \vdots \\ \|\boldsymbol{a}_{N_a}\|_2^2 \end{bmatrix} \mathbf{1}_{N_u}^T \in \mathbb{R}^{N_a\times N_u},$$

$$\underline{\mathbf{U}} = \mathbf{1}_{N_a}\begin{bmatrix} \|\boldsymbol{u}_1\|_2^2 & \|\boldsymbol{u}_2\|_2^2 & \cdots & \|\boldsymbol{u}_{N_u}\|_2^2 \end{bmatrix} \in \mathbb{R}^{N_a\times N_u}.$$

Accordingly, based on the discussions above, we can conclude that both $\underline{\mathbf{A}}$ and $\underline{\mathbf{U}}$ are rank-1 matrices. As $\mathbf{A}$ and $\mathbf{U}$ are rank-D matrices, $\mathbf{A}^T\mathbf{U}$ is a matrix with rank at most D. It can be found that the rank of $\mathbf{S}_{au}$ is at most $D+2$, which indicates that it is a low rank matrix as well.

Based on the theory of matrix correlation, a low rank matrix has fewer linearly independent rows or columns than its dimensions, and some of its rows or columns can be represented as a linear combination of the other rows or columns. Therefore, we can infer that it is feasible to recover $\mathbf{S}$ or its sub-matrices from sparse measurements.

C. Low Rank Matrix Completion

In practice, each WSN node has its own measurable communication radius R owing to the limited transmitting power and signal reception capability. The ranging measurements are no longer applicable when $d_{ij} > R$. Thus, after arranging the measurable ranges (in-radius) in SEDM, we can divide all the pairwise communication links into two parts: in-radius set $\mathcal{I}$ and out-of-radius set $\mathcal{O}$, given by

$$(i,j) \in \begin{cases} \mathcal{I} & \text{if } d_{ij} \leq R \\ \mathcal{O} & \text{if } d_{ij} > R. \end{cases} \tag{13}$$

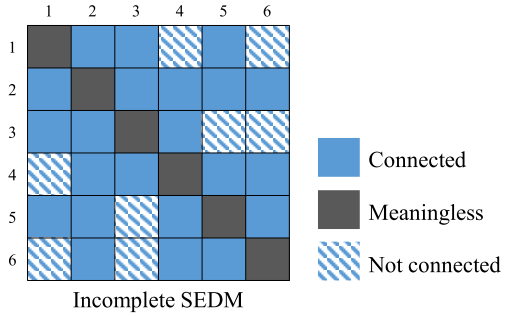

Fig. 2. Connectivity index table of the SEDM.

An example of describing the connectivity of the SEDM is shown in Fig. 2, the blue blocks stand for the measured pairwise distances, the gray blocks are meaningless and always equal to 0, and the stripe blocks stand for the missing ranging measurements. With the division of $\mathcal{I}$ and $\mathcal{O}$, we define the orthogonal mapping $\mathcal{P}$ of $\mathbf{S}$:

$$[\mathcal{P}]_{ij} = \begin{cases} 1 & (i,j) \in \mathcal{I} \\ 0 & (i,j) \in \mathcal{O}. \end{cases} \tag{14}$$

Then the problem turns to how to recover the SEDM by minimizing the following cost function:

$$\begin{aligned} \min \quad & \text{rank}(\hat{\mathbf{S}}) \\ \text{s.t.} \quad & \mathcal{P} \odot \hat{\mathbf{S}} = \mathcal{P} \odot \widetilde{\mathbf{S}} \\ & [\hat{\mathbf{S}}]_{ij} \geq R^2, (i,j) \in \mathcal{O}. \end{aligned} \tag{15}$$

To solve this problem, we refer the readers to Section I, where we reviewed the approximation and simplification of rank minimization in the literature. In this section, we briefly illustrate it with respect to formulations. It is known that $\text{rank}(\cdot)$ is a non-convex function [45, page 3], which makes (15) non-convex. Moreover, $\text{rank}(\mathbf{S})$ equals to the number of non-zero singular values, and thus (15) can be approximated by the convex envelope of $\text{rank}(\mathbf{S})$, i.e. nuclear norm $\|\hat{\mathbf{S}}\|_*$ [46]:

$$\begin{aligned} \min \quad & \|\hat{\mathbf{S}}\|_* \\ \text{s.t.} \quad & \mathcal{P} \odot \hat{\mathbf{S}} = \mathcal{P} \odot \widetilde{\mathbf{S}} \\ & [\hat{\mathbf{S}}]_{ij} \geq R^2, (i,j) \in \mathcal{O}, \end{aligned} \tag{16}$$

where $\|\hat{\mathbf{S}}\|_* = \sum_k \sigma_{s,k}$ and $\sigma_{s,k}$ is the singular value of $\hat{\mathbf{S}}$.

Accordingly, for a PSD and squared matrix, trace minimization is equivalent to nuclear norm minimization [27]

$$\begin{aligned} \min \quad & \text{Tr}(\hat{\mathbf{S}}) \\ \text{s.t.} \quad & \mathcal{P} \odot \hat{\mathbf{S}} = \mathcal{P} \odot \widetilde{\mathbf{S}} \\ & [\hat{\mathbf{S}}]_{ij} \geq R^2, (i,j) \in \mathcal{O}. \end{aligned} \tag{17}$$

However, as both the SEDM and $\mathbf{S}_{au}$ are non-PSD, (17) is not feasible in this case. We introduce the following lemma to minimize the rank of general matrices.

Lemma 1: For a matrix $\mathbf{M} \in \mathbb{R}^{m\times n}$, $\text{rank}(\mathbf{M}) \leq r$ *if and only if* $\mathbf{Y} = \mathbf{Y}^T \in \mathbb{R}^{m\times m}$ *and* $\mathbf{Z} = \mathbf{Z}^T \in \mathbb{R}^{n\times n}$ *s.t.*

$$\text{rank}\begin{pmatrix} \mathbf{Y} & \mathbf{0} \\ \mathbf{0} & \mathbf{Z} \end{pmatrix} \leq 2r, \begin{bmatrix} \mathbf{Y} & \mathbf{M} \\ \mathbf{M}^T & \mathbf{Z} \end{bmatrix} \succeq 0. \tag{18}$$

where $r \in \mathbb{R}$ *is a variable.*

Proof: See [27]. □

According to Lemma 1, when $\begin{bmatrix}\mathbf{Y} & \hat{\mathbf{S}}\\ \hat{\mathbf{S}}^T & \mathbf{Z}\end{bmatrix}$ is PSD, minimizing the rank of $\hat{\mathbf{S}}$ is equivalent to minimizing the rank of $\begin{bmatrix}\mathbf{Y} & \hat{\mathbf{S}}\\ \hat{\mathbf{S}}^T & \mathbf{Z}\end{bmatrix}$. Therefore, (17) can be converted to a trace minimization problem of PSD matrix $\begin{bmatrix}\mathbf{Y} & \hat{\mathbf{S}}\\ \hat{\mathbf{S}}^T & \mathbf{Z}\end{bmatrix}$, given by

$$\begin{aligned}\min\quad & \mathrm{Tr}\begin{pmatrix}\mathbf{Y} & \mathbf{0}\\ \mathbf{0} & \mathbf{Z}\end{pmatrix}\\ \text{s.t.}\quad & \begin{bmatrix}\mathbf{Y} & \hat{\mathbf{S}}\\ \hat{\mathbf{S}}^T & \mathbf{Z}\end{bmatrix}\succeq 0\\ & \mathcal{P}\odot\hat{\mathbf{S}}=\mathcal{P}\odot\widetilde{\mathbf{S}}\\ & [\hat{\mathbf{S}}]_{ij}\geq R^2,(i,j)\in\mathcal{O}.\end{aligned}\tag{19}$$

As for those low rank but not PSD matrices $\mathbf{S}$, their LRMC problem (19) can be treated as

$$\begin{aligned}\min\quad & t\\ \text{s.t.}\quad & \mathrm{Tr}(\mathbf{Y})+\mathrm{Tr}(\mathbf{Z})\leq 2t\\ & \begin{bmatrix}\mathbf{Y} & \hat{\mathbf{S}}\\ \hat{\mathbf{S}}^T & \mathbf{Z}\end{bmatrix}\succeq 0\\ & \mathcal{P}\odot\hat{\mathbf{S}}=\mathcal{P}\odot\widetilde{\mathbf{S}}\\ & [\hat{\mathbf{S}}]_{ij}\geq R^2,(i,j)\in\mathcal{O}.\end{aligned}\tag{20}$$

D. Positioning

By exploiting the recovered SEDM, the positioning accuracy of the unknown sensors can be improved. Regarding the completed squared distance $\hat{s}_{ij}$ and anchor position $\boldsymbol{a}_i$, the positioning problem can be reformulated as follows:

$$\min \sum_{(i,j)\in\mathcal{C}_{au}}\left\|\|\boldsymbol{a}_i-\boldsymbol{u}_j\|_2^2-\hat{s}_{ij}\right\|_2^2+\sum_{(i,j)\in\mathcal{C}_{uu}}\left\|\|\boldsymbol{u}_i-\boldsymbol{u}_j\|_2^2-\hat{s}_{ij}\right\|_2^2.\tag{21}$$

Replacing $\boldsymbol{u}_i$ by the position matrix $\mathbf{U}$, then we have

$$\|\boldsymbol{a}_i-\boldsymbol{u}_j\|_2^2=\left[\boldsymbol{e}_j^T,-\boldsymbol{a}_i^T\right]\begin{bmatrix}\mathbf{F} & \mathbf{U}^T\\ \mathbf{U} & \mathbf{I}\end{bmatrix}\begin{bmatrix}\boldsymbol{e}_j\\ -\boldsymbol{a}_i\end{bmatrix},\tag{22}$$

$$\|\boldsymbol{u}_i-\boldsymbol{u}_j\|_2^2=\left[\boldsymbol{e}_{ij}^T,\mathbf{0}_D^T\right]\begin{bmatrix}\mathbf{F} & \mathbf{U}^T\\ \mathbf{U} & \mathbf{I}\end{bmatrix}\begin{bmatrix}\boldsymbol{e}_{ij}\\ \mathbf{0}_D\end{bmatrix},\tag{23}$$

where $\mathbf{F}=\mathbf{U}^T\mathbf{U}\in\mathbb{R}^{N\times N}$. $\boldsymbol{e}_{ij}\in\mathbb{R}^{N_u\times 1}$ is a vector with 1 of the i^{th} element, -1 of the j^{th} element and zero everywhere else. For example, $\boldsymbol{e}_{14}=\begin{bmatrix}1&0&0&-1\end{bmatrix}^T$ when $N_u=4$. And $\boldsymbol{e}_j\in\mathbb{R}^{N_u\times 1}$ is the vector with 1 at the jth row and zero everywhere else. For example, $\boldsymbol{e}_3=\begin{bmatrix}0&0&1&0\end{bmatrix}^T$ when $N_u=4$. Then (21) can be rewritten as

$$\min \sum_{(i,j)\in\mathcal{C}_{au}}\left\|\left[\boldsymbol{e}_j^T,-\boldsymbol{a}_i^T\right]\mathbf{H}\begin{bmatrix}\boldsymbol{e}_j\\ -\boldsymbol{a}_i\end{bmatrix}-\hat{s}_{ij}\right\|_2^2+\sum_{(i,j)\in\mathcal{C}_{uu}}\left\|\left[\boldsymbol{e}_{ij}^T,\mathbf{0}_D^T\right]\mathbf{H}\begin{bmatrix}\boldsymbol{e}_{ij}\\ \mathbf{0}_D\end{bmatrix}-\hat{s}_{ij}\right\|_2^2,\tag{24}$$

where we define $\mathbf{H}=\begin{bmatrix}\mathbf{F} & \mathbf{U}^T\\ \mathbf{U} & \mathbf{I}\end{bmatrix}$.

Introduce the auxiliary variables $[\mathbf{B}]_{ij}$, (24) can be evolved into

$$\begin{aligned}\min\quad & \|\mathbf{B}\|_F\\ \text{s.t.}\quad & \left[\boldsymbol{e}_j^T,-\boldsymbol{a}_i^T\right]\mathbf{H}\begin{bmatrix}\boldsymbol{e}_j\\ -\boldsymbol{a}_i\end{bmatrix}-\hat{s}_{ij}\leq[\mathbf{B}]_{ij},(i,j)\in\mathcal{C}_{au}\\ & \left[\boldsymbol{e}_{ij}^T,\mathbf{0}_D^T\right]\mathbf{H}\begin{bmatrix}\boldsymbol{e}_{ij}\\ \mathbf{0}_D\end{bmatrix}-\hat{s}_{ij}\leq[\mathbf{B}]_{ij},(i,j)\in\mathcal{C}_{uu}.\end{aligned}\tag{25}$$

However, since $\mathbf{F}=\mathbf{U}^T\mathbf{U}$ is not a convex constraint, we relax such constraint by

$$\mathbf{F}\succeq\mathbf{U}^T\mathbf{U}.\tag{26}$$

A step further, by applying Schur complements, (26) is equivalent to [47]

$$\mathbf{H}\succeq 0.\tag{27}$$

Therefore, the cooperative positioning can be considered as a semi-definite relaxation programming, given by

$$\begin{aligned}\min\quad & \|\mathbf{B}\|_F\\ \text{s.t.}\quad & \left[\boldsymbol{e}_j^T,-\boldsymbol{a}_i^T\right]\mathbf{H}\begin{bmatrix}\boldsymbol{e}_j\\ -\boldsymbol{a}_i\end{bmatrix}-\hat{s}_{ij}\leq[\mathbf{B}]_{ij},(i,j)\in\mathcal{C}_{au}\\ & \left[\boldsymbol{e}_{ij}^T,\mathbf{0}_D^T\right]\mathbf{H}\begin{bmatrix}\boldsymbol{e}_{ij}\\ \mathbf{0}_D\end{bmatrix}-\hat{s}_{ij}\leq[\mathbf{B}]_{ij},(i,j)\in\mathcal{C}_{uu}\\ & \mathbf{H}\succeq 0.\end{aligned}\tag{28}$$

The relaxation operation in (26) can convert the non-convex problem (7) to the convex problem (28), which has a unique minimal solution and the solution can be obtained by the standard convex optimization frameworks [12]. For instance, the open source solvers SDPT3 and SeDuMi adopt the interior-point method to perform convex optimization [48].

III. Completion on the Graph

The discussions mentioned above aim to achieve cooperative positioning by solving the classic low rank problem. The classic LRMC problem, take (20) for instance, implies an assumption that the row and/or vectors are unorganized [18]. However, there exists a potential relationship between the vectors of SEDM, which can be explained by the simple scenario as follows. Assuming a series of nodes distributing in a space and measuring pairwise distances to all sensors, then one can get a pairwise distance vector to form $\mathbf{S}_{au}$. The distance vectors are represented by $\boldsymbol{\alpha}_i=[\mathbf{S}_{au}]_{i\cdot}$ and $\boldsymbol{\beta}_j=[\mathbf{S}_{au}]_{\cdot j}$. Take Fig. 3 for instance, the 2^{nd} sensor and the 4^{th} sensor are close in the Euclidean coordinate system, the 2^{nd} sensor and the 7^{th} sensor are connected but the 4^{th} sensor and the 7^{th} are unconnected. Therefore, we can approximately estimate d_{47} by using the visible ranging information d_{27}. Similarly, the measured ranges of the 11^{st} sensor and the 12^{nd} sensor are close, and thus we can infer that $\boldsymbol{\alpha}_{11}\approx\boldsymbol{\alpha}_{12}$ and $\boldsymbol{\beta}_{11}\approx\boldsymbol{\beta}_{12}$. On the other hand, as the relative distance of the 10^{th} sensor is further than that of the 12^{nd} sensor, its weight is relatively smaller. In a word, a closer pair of nodes results in more correlated ranging measurements. In this section, we proposed a novel LRMC positioning scheme that take both the low rank property and correlation between vectors into account, as shown in Fig. 4. We represent the sensor correlation by undirected weighted graphs, and then

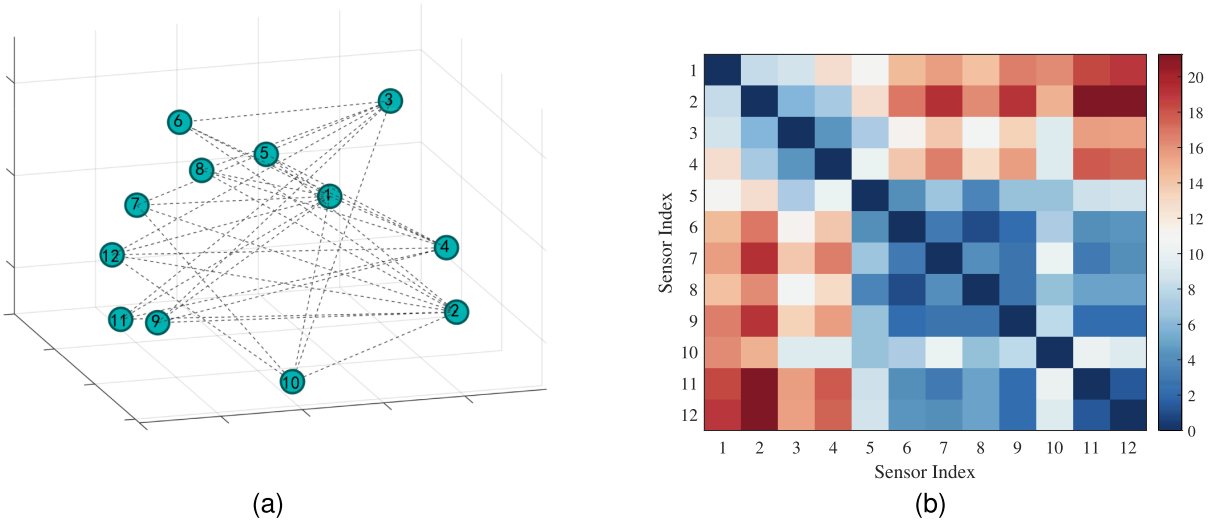

Fig. 3. An example of a WSN with $N = 12$ nodes showing sensor correlation. (a) Topology of this network, where the circles represent the member sensor nodes, and the lines represent the communication links. (b) EDM vector correlation, where short distances are shown in dark blue, medium distances are shown in white and long distances are shown in red.

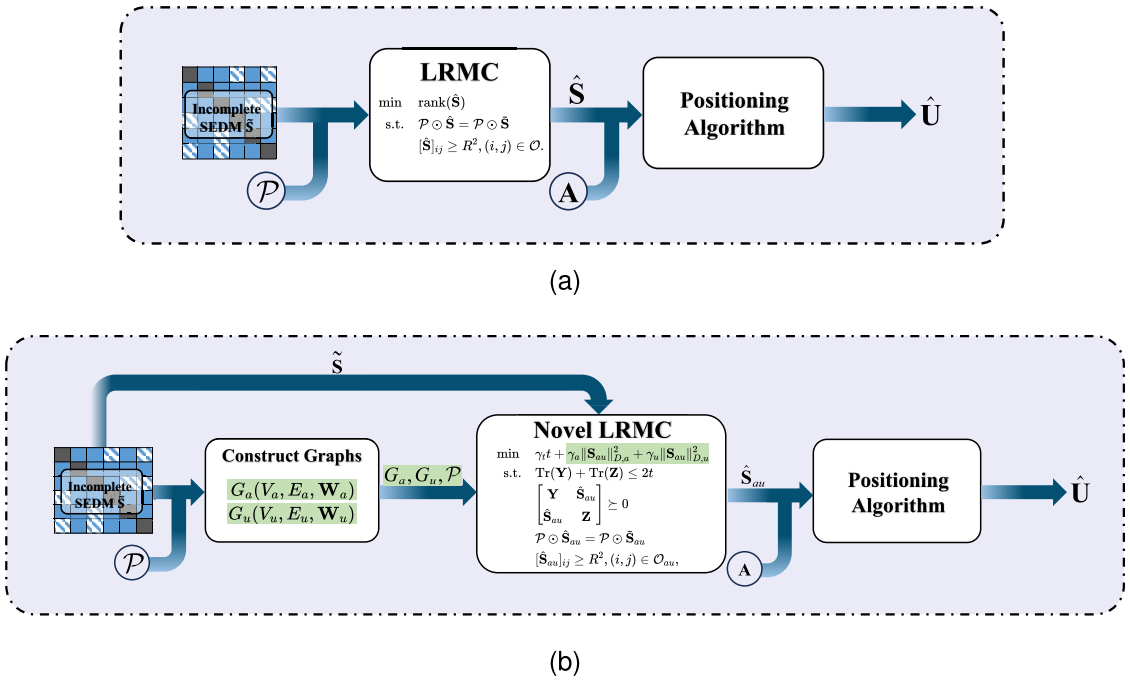

Fig. 4. Comparison of (a) the classic LRMC positioning scheme and (b) the proposed LRMC positioning scheme.

quantify them by Laplacian of graphs to incorporate it into the minimization problem and enable the solution to be smooth on the graph/manifold.

A. Graph of Sensor Correlation

Based on the discussions above, we can infer that the ranging measurements correlation might contribute to the SEDM completion. For this reason, we use indirect weighted graphs to indicate the correlation.

We construct the undirected weighted sensor graphs and use Laplacian to quantify the correlation of ranging measurements, namely, column and row correlation of EDM/SEDM. Define the anchor graph $G_a = (V_a, E_a, \mathbf{W}_a)$ with vertices $V_a = \{1, \cdots, N_a\}$ and edges $E_r = V_a \times V_a$ weighted with a weight matrix $\mathbf{W}_a \in \mathbb{R}^{N_a \times N_a}$. Since we assume that all the pairwise distances of anchors are known, G_a is a complete graph.

In this paper, the edge weights stand for the vertices correlation of weighted graphs, which indicates that closer sensor pairs lead to more correlated vectors. We use d_{ij}^{-1} to weight the edge, given by

$$[\mathbf{W}_a]_{ij} = \begin{cases} d_{ij}^{-1} & \text{if } i \neq j \\ 0 & \text{otherwise.} \end{cases} \tag{29}$$

We use the Laplacian to make the function smooth on the graphs. In theory, Laplacian is able to find a low-dimensional manifold of a high-dimensional vector that preserves the distribution characteristics of the data [40]. The quadratic form of graph Laplacian is the sum of the squared differences between the signals on any two edges of the graph

$$\varphi_{ij}^{a} \triangleq \sum_{i,j} \|\boldsymbol{\alpha}_i - \boldsymbol{\alpha}_j\|_2^2. \tag{30}$$

In this paper, we use the Laplacian of anchor graph to quantify the correlated relationship of distance vectors measured by the anchors, given by

$$\begin{aligned}\|\mathbf{S}_{au}\|_{D,a}^2 &\triangleq \frac{1}{2}\sum_{i,j} w_{ij}^{a}\varphi_{ij}^{a} \\ &= \sum_{ij} \boldsymbol{\alpha}_i w_{ij}^{a} \boldsymbol{\alpha}_i^T - \sum_{ij} \boldsymbol{\alpha}_i w_{ij}^{a} \boldsymbol{\alpha}_j^T \\ &= \sum_{i} \boldsymbol{\alpha}_i [\mathbf{Q}_a]_{ii} \boldsymbol{\alpha}_i^T - \mathbf{S}_{au}\mathbf{W}_a\mathbf{S}_{au}^T \\ &= \mathbf{S}_{au}\mathbf{Q}_a\mathbf{S}_{au}^T - \mathbf{S}_{au}\mathbf{W}_a\mathbf{S}_{au}^T \\ &= \mathbf{S}_{au}(\mathbf{Q}_a - \mathbf{W}_a)\mathbf{S}_{au}^T,\end{aligned} \tag{31}$$

where $w_{ij}^{a} = [\mathbf{W}_a]_{ij}$ is the weight of edge (i,j), $\mathbf{Q}_a$ denotes the degree matrix that contains the degrees of the vertices along the diagonal:

$$[\mathbf{Q}_a]_{ij} = \begin{cases} \sum_{j=1}^{N_a} w_{ij}^{a} & \text{if } i = j \\ 0 & \text{otherwise.} \end{cases} \tag{32}$$

Define $\mathbf{L}_a = \mathbf{Q}_a - \mathbf{W}_a$ as the Laplacian matrix:

$$\|\mathbf{S}_{au}\|_{D,a}^2 = \mathrm{Tr}(\mathbf{S}_{au}\mathbf{L}_a\mathbf{S}_{au}^T). \tag{33}$$

It is worth noting that both $\mathbf{L}_a$ and $\mathbf{L}_u$ are PSD, so we can infer that $\|\mathbf{S}_{au}\|_{D,a}^2 \geq 0$ when the weights are non-negative.

We assume the close sensors measure similar distance vectors, i.e. let Laplacian $\|\mathbf{S}_{au}\|_{D,a}^2$ of G_a be small. Inspired by manifold learning, the minimization of the Laplacian force the function to be smooth in the manifold.

Follow the same line, since we collected a number of pairwise distances among unknown sensors, we can construct an unknown sensor graph $G_u = (V_u, E_u, \mathbf{W}_u)$ with vertices $V_u = \{N_a + 1, \cdots, N_a + N_u\}$. Different from G_a, the incomplete measurements result in an sub-edge set, i.e. $E_u \subseteq V_u \times V_u$. As the edge set E_u represents the connected pair set $(i,j) \in \mathcal{C}_{uu}$, where $\mathcal{C}_{uu} = \{(i,j) \mid \|\boldsymbol{u}_i - \boldsymbol{u}_j\|_2 \leq R\}$, we can infer that G_u is not a complete graph. The Laplacian of unknown sensor graph G_u is

$$\begin{aligned}\|\mathbf{S}_{au}\|_{D,u}^2 &\triangleq \sum_{i,j} w_{ij}^{u}\varphi_{ij}^{u} \\ &= \mathrm{Tr}(\mathbf{S}_{au}\mathbf{L}_u\mathbf{S}_{au}^T),\end{aligned} \tag{34}$$

where $w_{ij}^{u} = [\mathbf{W}_u]_{ij}$ is the weight of edge (i,j), $\varphi_{ij}^{u} = \|\boldsymbol{\beta}_i - \boldsymbol{\beta}_j\|_2^2$ is the squared differences on edges of the unknown sensor graph. $\mathbf{L}_u = \mathbf{Q}_u - \mathbf{W}_u$ and $\mathbf{Q}_u$ is the degree matrix

$$[\mathbf{Q}_u]_{ij} = \begin{cases} \sum_{j=1}^{N_u} w_{ij}^{u} & \text{if } i = j \\ 0 & \text{otherwise.} \end{cases} \tag{35}$$

Similarly, $\|\mathbf{S}_{au}\|_{D,u}^2$ should be as small as possible when the communication links among unknown sensors are visible.

B. Proposed LRMC Method

By taking the feature of sensor correlation (33) and (34) into account, the LRMC presented in (20) can be considered as a multi objective optimization problem. It is feasible to use the linear weighting method to tackle this problem, given by

$$\begin{aligned}\min \quad & \gamma_t t + \gamma_a \|\hat{\mathbf{S}}_{au}\|_{D,a}^2 + \gamma_u \|\hat{\mathbf{S}}_{au}\|_{D,u}^2 \\ \text{s.t.} \quad & \mathrm{Tr}(\mathbf{Y}) + \mathrm{Tr}(\mathbf{Z}) \leq 2t \\ & \begin{bmatrix} \mathbf{Y} & \hat{\mathbf{S}}_{au} \\ \hat{\mathbf{S}}_{au} & \mathbf{Z} \end{bmatrix} \succeq 0 \\ & \mathcal{P} \odot \hat{\mathbf{S}}_{au} = \mathcal{P} \odot \widetilde{\mathbf{S}}_{au} \\ & [\hat{\mathbf{S}}_{au}]_{ij} \geq R^2, (i,j) \in \mathcal{O}_{au},\end{aligned} \tag{36}$$

where $\mathcal{O}_{au} = \{(i,j) \mid \|\boldsymbol{a}_i - \boldsymbol{u}_j\|_2 \geq R\}$ denotes the set of invisible pairs between anchor nodes and sensor nodes, and $\gamma_t, \gamma_a, \gamma_u$ are the hyper-parameters controlling the corresponding objectives, respectively. All the objective functions of (36) are convex and closed, and thus this problem can be solved by CVX.

Consider that we can get other information of anchors and unknown sensors to construct G_a and G_u, here we complete $\mathbf{S}_{au}$ instead of $\mathbf{S}$. This completion method is flexible to different kinds of graph construction model, especially when constructing G_a and G_u by other types of information instead of range-only measurements. Furthermore, it should be noted that the SDP estimator based on partial links $\hat{\mathbf{S}}_{au}$ has lower complexity than those estimators based on the entire links $\hat{\mathbf{S}}$ due to the reduced number of constraints.

C. Proposed Positioning Method

In this section, we localize the unknown sensors with the completed distance matrix $\mathbf{S}_{au}$. Regarding the completed square distances and anchor positions, the positioning problem can be reformulated as follows:

$$\min \sum_{(i,j)\in\mathcal{C}_{au}} \left\| \|\boldsymbol{a}_i - \boldsymbol{u}_j\|_2^2 - \hat{s}_{ij} \right\|_2^2. \tag{37}$$

Substituting (22) into (37) yields

$$\min \sum_{(i,j)\in\mathcal{C}_{au}} \left\| [\boldsymbol{e}_j^T, -\boldsymbol{a}_i^T]\, \mathbf{H} \begin{bmatrix} \boldsymbol{e}_j \\ -\boldsymbol{a}_i \end{bmatrix} - \hat{s}_{ij} \right\|_2^2. \tag{38}$$

Follow the relaxation from (24) to (28), we relax the objective function of (37) by letting $\mathbf{H} \succeq 0$ and $[\boldsymbol{e}_j^T, -\boldsymbol{a}_i^T]\, \mathbf{H} \begin{bmatrix} \boldsymbol{e}_j^T \\ -\boldsymbol{a}_i^T \end{bmatrix} - \hat{s}_{ij} \leq [\mathbf{B}]_{ij}$. Then the SDP-based cooperative positioning can be relaxed as

$$\begin{aligned}\min \quad & \|\mathbf{B}\|_F \\ \text{s.t.} \quad & [\boldsymbol{e}_j^T, -\boldsymbol{a}_i^T]\, \mathbf{H} \begin{bmatrix} \boldsymbol{e}_j^T \\ -\boldsymbol{a}_i^T \end{bmatrix} - \hat{s}_{ij} \leq [\mathbf{B}]_{ij}, (i,j) \in \mathcal{C}_{au} \\ & \mathbf{H} \succeq 0.\end{aligned} \tag{39}$$

Similar to (36), (39) can also be solved by CVX.

In summary, our approach comprises two steps. At the first step, we construct the sensor graphs, which consist of anchor graph G_a and unknown sensor graph G_u to quantify the sensor measurement vector correlation by the distance. Then at the second step, we use the Laplacian and trace heuristic to

Algorithm 1 Proposed LRMC-Based Positioning Algorithm

Require: Incomplete SEDM $\widetilde{\mathbf{S}}$, orthogonal mapping $\mathcal{P}$, anchor positions $\mathbf{A}$, communication radius R, number of anchors N_a and unknown sensors N_u

Initialization

Assign empty vertexes sets V_a, V_u, edges sets E_a, E_u and weight matrices $\mathbf{W}_a, \mathbf{W}_u$ to anchor graph G_a and unknown sensor graph G_u, respectively, i.e. let $G_a = (V_a, E_a, \mathbf{W}_a)$ and $G_u = (V_u, E_u, \mathbf{W}_u)$

Construct anchor graph

for $i = 1$ to N_a **do**
  for $j = 1$ to N_a **do**
    if $[\mathcal{P}]_{ij} = 1$ **then**
      Add vertex i and j to vertexes set V_a
      Add edge $\{i, j\}$ to edges set E_a
      Add weight $[\mathbf{W}_a]_{ij} = 1/d_{ij}$
    end if
  end for
end for

Construct unknown sensor graph

for $i = N_a + 1$ to N **do**
  for $j = N_a + 1$ to N **do**
    if $[\mathcal{P}]_{ij} = 1$ **then**
      Add vertex i and j to vertexes set V_u
      Add edge $\{i, j\}$ to edges set E_u
      Add weight $[\mathbf{W}_u]_{ij} = 1/d_{ij}$
    end if
  end for
end for

Construct degree matrix $\mathbf{Q}_a$ as (32) and $\mathbf{Q}_u$ as (35)

Calculate Laplacian matrix, i.e. $\mathbf{L}_a = \mathbf{Q}_a - \mathbf{W}_a$ and $\mathbf{L}_u = \mathbf{Q}_u - \mathbf{W}_u$

Complete $\mathbf{S}_{au}$ according to (36)

Localize the unknown sensors according to (39)

complete the matrix on sensor graphs. An illustrative representation of the proposed LRMC-based positioning algorithm is shown in Algorithm 1.

IV. Simulations

Simulations are conducted to evaluate the performance of the proposed algorithm in this section. The proposed LRMC algorithm is evaluated in comparison to the existing LRMC algorithms TNNR-ADMM [35], TFOCS [49] and SDP-based LRMC algorithm proposed by [8] and [20] (labeled as SDP-C). Since the proposed algorithm is able to recover the sub-matrix $\mathbf{S}_{au}$, we give the comparison of completion performance with respect to $\mathbf{S}_{au}$. As for the algorithms that employ more observations contribute to the completion accuracy, we complete $\mathbf{S}$ and then analyze $\mathbf{S}_{au}$. The proposed positioning algorithm is compared with the conventional positioning algorithms MDS [1], universal cooperative localizer (UCL) [4][1] and SDP-based positioning algorithm proposed by [20] (labeled as SDP-P). The classic MDS is coupled with a rotation-translation transformation [50] (labeled as MDS-A) so that the relative positions can be mapped into the reference coordinate system provided by anchor nodes. All simulations presented are averaged over 400 independent Monte Carlo runs.

We consider a network of $N_a = 5$ anchors and $N_u = 6$ unknown sensors, one can infer that $\mathbf{S}_{au} \in \mathbb{R}^{5\times 6}$ is a low rank matrix according to the discussions in Section II. All the sensors are assumed to be capable of ranging with each other in the communication radius. The pairwise distances are measured by TOA or RSS, and all the communication links are independent of each other. The positions of anchors are given by

$$\mathbf{A} = \begin{bmatrix} 10 & 10 & -10 & -10 & 8 \\ 10 & -10 & 10 & -10 & 8 \end{bmatrix}. \tag{40}$$

The unknown sensors are randomly distributed in the range of 20 m $\times$20 m. The average denied rates are given by

$$\text{rate}(R) = \frac{|\mathcal{O}|}{N^2 - N_a^2 - N_u}\%, \tag{41}$$

where $|\mathcal{O}|$ denotes the number of node pairs in the out-of-radius set $\mathcal{O}$ (defined in (13)). We ignore N_u diagonal elements since the diagonal of $\mathbf{S}_{uu}$ is meaningless, and N_a^2 elements of $\mathbf{S}_{aa}$ are also disregarded since they are assumed to be known. The average denied rates versus radius (R) are shown in Table I. As discussed in (2) and (4), the TOA ranging noise and the RSS noise are setup as independent Gaussian white noise with zero means and variance σ and σ_r, respectively. The values of σ, σ_r and R will be stated in the following simulations. We present the simulation results and conduct for two ranging techniques, respectively.

A. Evaluation Metric

Refer to [20], LRMC algorithms are evaluated by relative completion error (RCE) and positioning algorithms are evaluated by root mean square error (RMSE). RCE is given by

$$\text{RCE}(\mathbf{D}_{au}) = N_{mc}^{-1} \sum_{n=1}^{N_{mc}} \frac{\|\hat{\mathbf{D}}_{au}(n) - \mathbf{D}_{au}\|_F}{\|\mathbf{D}_{au}\|_F}, \tag{42}$$

where $\hat{\mathbf{D}}_{au}(n)$ denotes the n^{th} estimate of the incomplete matrix $\mathbf{D}_{au}$, $N_{mc} = 400$ denotes the Monte Carlo runs and $n \in [1, N_{mc}]$.

Then RMSE is given by

$$\text{RMSE}(\mathbf{U}) = N_{mc}^{-1} \sum_{n=1}^{N_{mc}} \sqrt{\frac{\sum_{n=i}^{N_u} \|\hat{\boldsymbol{u}}_i(n) - \boldsymbol{u}_i\|_2^2}{N_u}}, \tag{43}$$

where $\hat{\boldsymbol{u}}_i(n)$ is the n^{th} estimate of the i^{th} sensor position $\boldsymbol{u}_i$ during N_{mc} Monte Carlo runs.

B. Varying Radius of TOA

To evaluate the performance of the proposed algorithm for varying radius, we let R vary from 12 m to 30 m. In practical, the accuracy of TOA measurement is in the order of centimeters when two sensors are in line of sight, or up to the order of meters with the presence of occlusion. The proposed algorithm is evaluated in two different scenarios with $\sigma = 0$ dB meter and $\sigma = -8$ dB meter, respectively.

[1]Refer to [4], we use the estimation of Ad hoc positioning system (APS) for the initialization of UCL. However, the generalized approximate message passing (GAMP) may not converge, UCL would diverge especially when R is low [6]. Therefore, we only present the results of UCL under appropriate conditions.

TABLE I
THE AVERAGE DENIED RATES FOR DIFFERENT RADIUS

Radius(m)	12	14	16	18	20	22	24	26	28	30
Denied rate(%)	61.0	49.3	38.4	26.4	15.2	7.6	3.8	1.3	0.1	0
Denied pairs	54	44	34	25	14	7	3.5	1	0.087	0
Degree per node	5.01	5.96	6.85	7.83	8.75	9.37	9.69	9.89	9.99	10.00

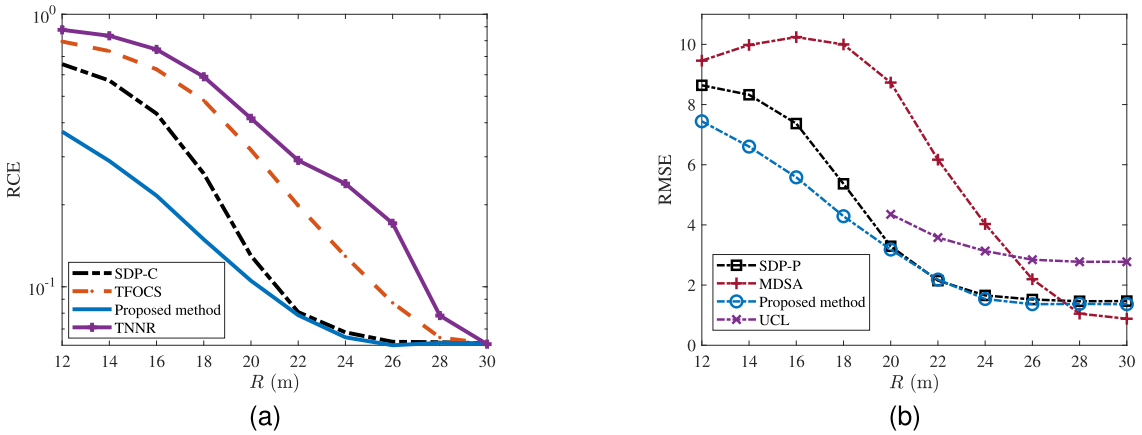

Fig. 5. (a) RCEs of SEDM completion and (b) RMSEs of positioning for varying radius with $\sigma = 0$ dB meter.

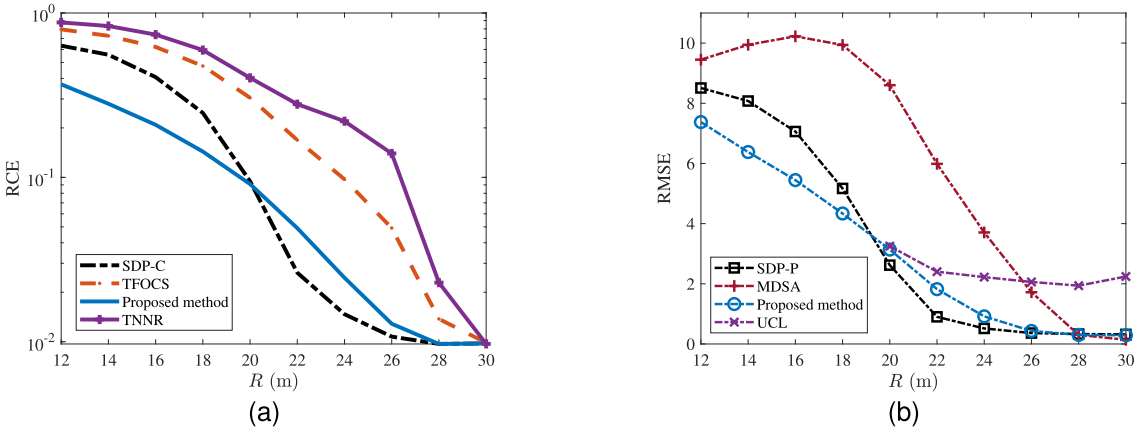

Fig. 6. (a) RCEs of SEDM completion and (b) RMSEs of positioning for varying radius with $\sigma = -8$ dB meter.

Fig. 5(a) shows the RCE of different completion algorithms with $\sigma = 0$ dB meter. The proposed algorithm slightly outperforms other algorithms when $R \in [12, 26]$ m and significantly outperforms when $R \in [12, 18]$ m since it benefits from incorporating the sensor correlation, namely Laplacian minimization. It should be noted that the sampling of SEDM subjected to the communication radius in this paper is non-uniform, which is an important reason that has a negative effect on the performance of other algorithms. Unlike these algorithms which exhibit excellent performance in uniform sampling scenario but degrade in non-uniform sampling scenario, the multi-objective cooperative filtering of the proposed algorithm consists of three components, and thus allowing it to clearly benefit from combining low rank property and sensor correlation. It can be seen that all the communication links are visible when $R = 30$ m, RCE($\mathbf{D}_{au}$)$=\sqrt{\sum_{i,j} \eta_{ij}^2}/\|\mathbf{D}_{au}\|_F$ in this case. That is to say, all the elements of SEDM can be measured so that the matrix recovery process is no longer required, the RCE originates from the measurement noise in this case. Additionally, it can be shown that both the measurement noise and estimation error of matrix recovery contribute to RCE when $R < 30$ m. When $R \in [22, 28]$ m, the RCE of the proposed algorithm is close to the RCE of SDP-C, which reveals the fact that the Laplacian of sensor graphs is small. The simulation results demonstrate that minimizing the Laplacian of sensor graphs is possible and rational. Incorporating the feature of sensor correlation improves the performance of LRMC. As expected, the accuracy of positioning and completion algorithms improve as the radius increases. Since the larger radius leads to higher connectivity and sampling rate, the accuracy of completion increase. Consequently, the performance of positioning improves due to more accurate distance estimation. As expected, UCL is inferior to SDP-P and the proposed method, since the simplified operation of generalized approximate message passing in [4] causes a slight performance degradation of UCL. Additionally, it can

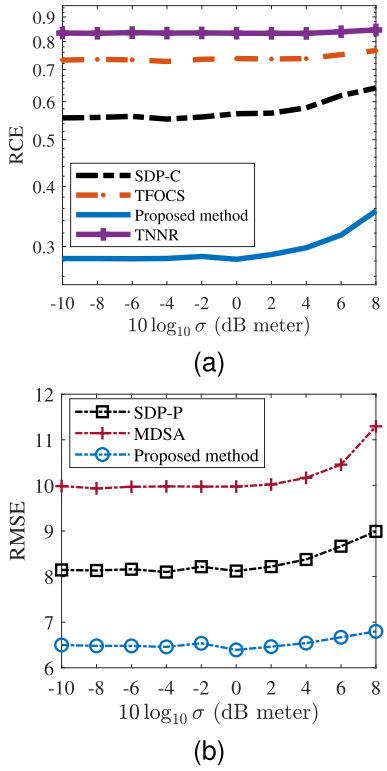

Fig. 7. (a) RCEs of SEDM completion and (b) RMSEs of positioning for varying noise with $R = 14$ m.

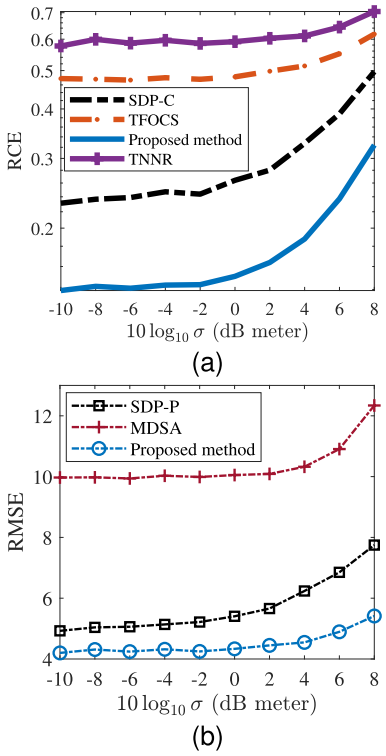

Fig. 8. (a) RCEs of SEDM completion and (b) RMSEs of positioning for varying noise with $R = 18$ m.

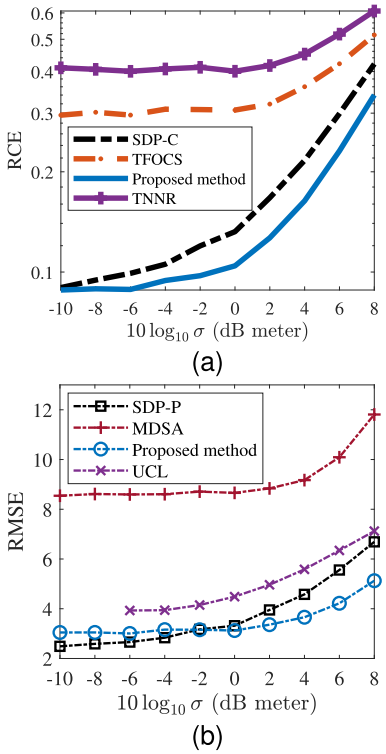

Fig. 9. (a) RCEs of SEDM completion and (b) RMSEs of positioning for varying noise with $R = 20$ m.

be observed that MDS-A slightly outperforms SDP-P and the proposed method when $R = 30$ m. The reason is that MDS-A retains rank constraint, i.e. $\text{rank}(\mathbf{S}) = P+2$, which is neglected in SDP-based algorithms [51], e.g. (39). Such a constraint enables MDS-A to achieve a better performance when the distance matrix has almost no missing elements.

The results for $\sigma = -8$ dB meter are displayed in Fig. 6. It shows that the proposed method and SDP-C outperform other algorithms. The proposed algorithm behaves better than SDP-C in low radius, whereas SDP-C works better in intermediate radius, and both of them are comparable in high radius. To achieve the best performance, the trace minimization theory requires that the indices of the observed entries are uniformly sampled [38]. However, challenges such as low signal-to-noise ratio and non-uniformly sampling are common in WSN applications. The stringent requirements of trace minimization, including uniform sampling and low level noise, severely limit its application scenarios. Thus, addressing this problem is one of our motivations. As shown in Fig. 5 and Fig. 7 $\sim$ Fig. 9, the proposed algorithm can still achieve a good performance in challenging scenarios. Moreover, similar to Fig. 5, it can be shown that the positioning performances presented in Fig. 7b $\sim$ Fig. 9b also behave better as the completion accuracy improves. The accuracy of relative position for MDS-A would be greatly decreased once there are missing items in SEDM. However, when the denied rates are extremely low, MDS-A performs better due to the rank constraint.

C. Varying Noise of TOA

We consider 3 scenarios with varying noise and conduct the corresponding results respectively to assess the impact of the signal-noise ratio (SNR). The simulated scenarios are setup as follows: 1) hard case with $R = 14$ m are setup with the presence of complex propagation environments where mutual occlusion and electromagnetic interference exist; 2) intermediate case with $R = 18$ m, in which we simulate a sparse WSN; 3) low case with $R = 20$ m where we simulate the dense

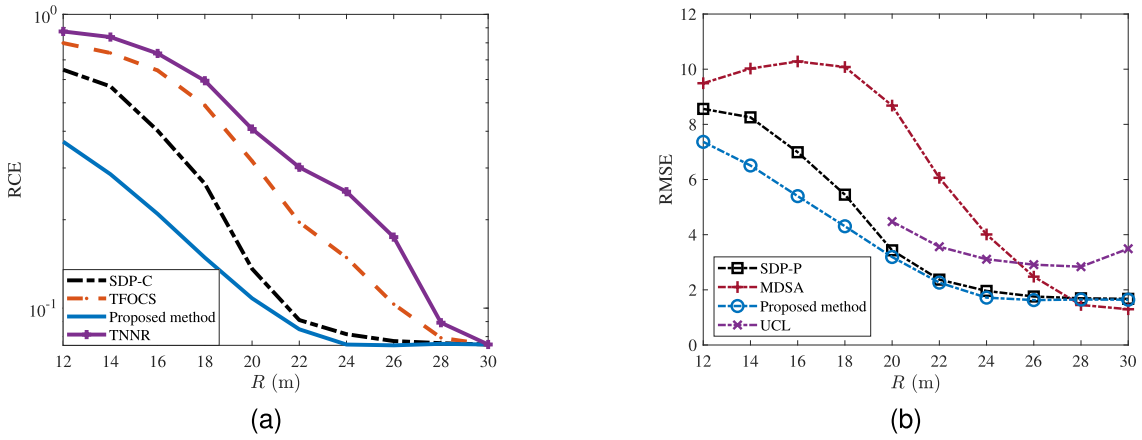

Fig. 10. (a) RCEs of SEDM completion and (b) RMSEs of positioning for varying radius with $\sigma_r = 0$ dB meter.

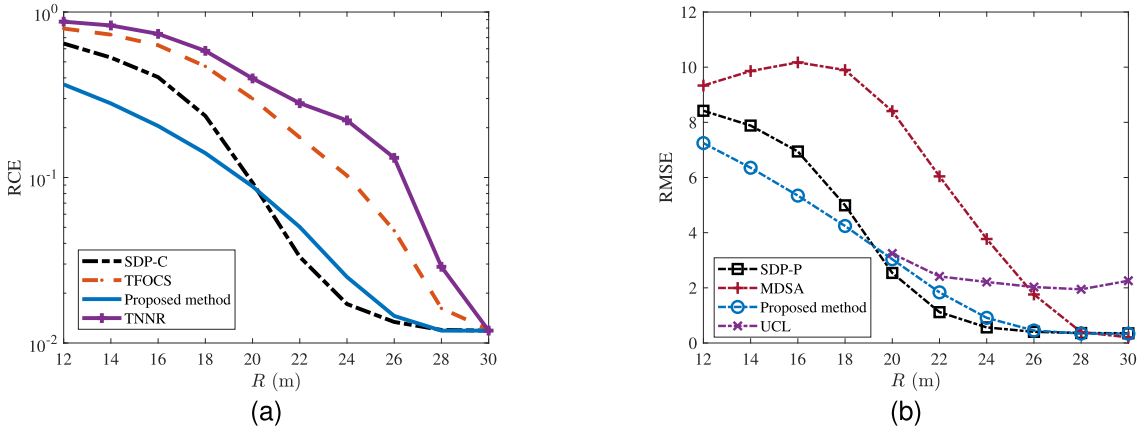

Fig. 11. (a) RCEs of SEDM completion and (b) RMSEs of positioning for varying radius with $\sigma_r = -8$ dB meter.

or LOS scenarios. As shown in Table I, their corresponding denied rates are 36.7%, 20.3% and 11.5%, respectively. The algorithms are then evaluated in a range of SNRs by varying σ in $[-10, 8]$ dB meter. The RCE of completion and RMSE of positioning are presented in Fig. 7, Fig. 8 and Fig. 9, respectively. Similar to the simulation in section IV-B, the accuracy of positioning improves as the RCE of completion increases. Since completion errors are the primary errors in the hard case, all RCE of algorithms retain a stable degree of accuracy when $\sigma \in [-10, 0]$ dB meter. This is in contrast to the results for the low case, intermediate case, and hard case when $\sigma \in [0, 8]$ dB meter. In these cases, the errors are caused by both noise and completion process, and thus the RCE is proportional to the SNR. In low case with high noise level, intermediate case and hard case, the proposed algorithm outperforms the other algorithms and maintains relative stable in RCE and RMSE. However, in low case with low noise level, although the proposed completion algorithm estimates more accurate SEDM, the positioning accuracy of the proposed algorithm is lower than SDP-P. The reason is that we utilize $\mathbf{S}_{au}$ which consists of less pairwise distance information to localize the sensors, while SDP-P uses $\mathbf{S}$.

D. Varying Noise of RSS

In this section, we assess the performance of the proposed algorithm based on RSS ranging in two scenarios: one with high SNR ($\sigma_r = -8$ dB meter) and one with low SNR ($\sigma_r = 0$ dB meter). It should be noted that the ranging error is proportional to the distance in RSS ranging, given by:

$$\widetilde{d}_{ij} = \frac{d_{ij}}{10^{q_{ij}/(10n_p)}}. \tag{44}$$

In contrast to TOA ranging, the ranging accuracy declines as the distance increases. The denied rates for varying R from 12 m to 30 m are presented in Table I. The RSS path loss model was presented in (4) and the related parameters are shown in Table II.

TABLE II
THE PARAMETERS OF RSS PATH LOSS MODEL FOR SIMULATIONS

Description	Symbol	Values
Path loss exponent	n_p	3
Reference distance	d_0	1
Received power of d_0	P_0	46

The results of $\sigma_r = 0$ dB meter are shown in Fig. 10, it can be found that the proposed algorithm presents similar performance with TOA ranging. Additionally, the proposed algorithm benefits from multi-objective cooperative filtering, particularly the Laplacian minimization, which makes it perform better than other algorithms when $R \in [12, 26]$ m and significantly outperform them when $R \in [12, 18]$ m. Fig. 11

TABLE III
THE AVERAGE RCE

Algorithm	The proposed algorithm	SDP-C	TNNR	TFOCS
RCE	**0.1094**	0.1206	0.3575	0.3102

TABLE IV
THE AVERAGE RMSE

Algorithm	The proposed algorithm	SDP-P	MDS-A
RMSE	**3.5460**	3.6253	7.5701

presents the results when $\sigma_r = -8$ dB meter. It can be seen that the proposed algorithm outperforms the other algorithms in both low and intermediate radius. In both 0 dB meter and -8 dB meter noise level, the increasing radius boosts the performance of completion algorithms and consequently improves the performance of the proposed algorithm and SDP-P.

E. Large Scale Network

In this subsection, we examine the performance of the proposed method in a large scale network, which consists of $N_a = 10$ anchors and $N_u = 50$ unknown sensors. All the nodes are randomly deployed within a range of 20 m $\times$20 m, and each of them employs two-way communication. We let the communication radius $R = 18$ m in this subsection. The adopted TOA ranging model is presented in (3), with $\sigma = 1$ m. The RCE of LRMC algorithms are presented in Table III. It can be seen that the proposed method outperforms other methods. Table IV shows the RMSE of the positioning algorithms. The proposed method also outperforms SDP-P and MDS-A. Additionally, compared with Fig. 8b which presents the RMSE of positioning algorithms in small scale networks, there is an improvement in positioning accuracy. The reason is that the nodes in the large scale network can collect more ranging measurements than those nodes in the small one. Nevertheless, the incomplete SEDM fails to meet the accuracy and integrity requirements of MDS-A, which results in a poor performance.

V. CONCLUSION

In this paper, we propose a novel cooperative positioning algorithm in complex propagation environments that combines LRMC and Laplacian regularization to effectively exploit the linear combination of rows/columns and the correlation information among sensors. We also present a SDP-based positioning algorithm which uses the recovered SEDM and anchor positions to accurately localize the unknown sensors. The simulation experiments show that the proposed algorithm outperforms other algorithms under different noise levels and communication radius. Meanwhile, the simulation experiments verify the feasibility of our assumption. The paper provides an effective and robust solution for the partial connectivity positioning problem in wireless sensor networks. One of the promising future direction is to develop a robust LRMC algorithm to enable RCE to be lower than noise level by relaxing the constraints on range measurements.

REFERENCES

[1] R. T. Rajan, G. Leus, and A.-J. van der Veen, "Joint relative position and velocity estimation for an anchorless network of mobile nodes," *Signal Process.*, vol. 115, pp. 66–78, Oct. 2015.

[2] Q. Shi, X. Cui, S. Zhao, S. Xu, and M. Lu, "BLAS: Broadcast relative localization and clock synchronization for dynamic dense multiagent systems," *IEEE Trans. Aerosp. Electron. Syst.*, vol. 56, no. 5, pp. 3822–3839, Oct. 2020.

[3] C. Di Franco, M. Marinoni, E. Bini, and G. C. Buttazzo, "Dynamic multidimensional scaling with anchors and height constraints for indoor localization of mobile nodes," *Robot. Auto. Syst.*, vol. 108, pp. 28–37, Oct. 2018.

[4] S. Wang and X. Jiang, "Three-dimensional cooperative positioning in vehicular ad-hoc networks," *IEEE Trans. Intell. Transp. Syst.*, vol. 22, no. 2, pp. 937–950, Feb. 2021.

[5] S. Wang, X. Jiang, and H. Wymeersch, "Cooperative localization in wireless sensor networks with AOA measurements," *IEEE Trans. Wireless Commun.*, vol. 21, no. 8, pp. 6760–6773, Aug. 2022.

[6] S. Wang, F. Luo, and L. Zhang, "Universal cooperative localizer for WSN with varied types of ranging measurements," *IEEE Signal Process. Lett.*, vol. 24, no. 8, pp. 1223–1227, Aug. 2017.

[7] F. Luo, S. Wang, Y. Gong, X. Jing, and L. Zhang, "Geographical information enhanced cooperative localization in vehicular ad-hoc networks," *IEEE Signal Process. Lett.*, vol. 25, no. 4, pp. 556–560, Apr. 2018.

[8] X. Guo, L. Chu, and X. Sun, "Accurate localization of multiple sources using semidefinite programming based on incomplete range matrix," *IEEE Sensors J.*, vol. 16, no. 13, pp. 5319–5324, Jul. 2016.

[9] S. Kumar, R. Kumar, and K. Rajawat, "Cooperative localization of mobile networks via velocity-assisted multidimensional scaling," *IEEE Trans. Signal Process.*, vol. 64, no. 7, pp. 1744–1758, Apr. 2016.

[10] Y. Fan, K. Ding, X. Qi, and L. Liu, "Cooperative localization of 3D mobile networks via relative distance and velocity measurement," *IEEE Commun. Lett.*, vol. 25, no. 9, pp. 2899–2903, Sep. 2021.

[11] P. Jiang, C. Zheng, Q. Ke, and X. Gu, "Robust cooperative localization using peer-to-peer ranging measurements," *Peer-to-Peer Netw. Appl.*, vol. 16, no. 5, pp. 2103–2112, Sep. 2023.

[12] P. Biswas and Y. Ye, "Semidefinite programming for ad hoc wireless sensor network localization," in *Proc. 3rd Int. Symp. Inf. Process. sensor Netw.*, Apr. 2004, pp. 46–54.

[13] P. Biswas and Y. Yinyu, "A distributed method for solving semidefinite programs arising from ad hoc wireless sensor network localization," in *Multiscale Optimization Methods and Applications*, 2006, pp. 69–84.

[14] P. Biswas, K.-C. Toh, and Y. Ye, "A distributed SDP approach for large-scale noisy anchor-free graph realization with applications to molecular conformation," *SIAM J. Sci. Comput.*, vol. 30, no. 3, pp. 1251–1277, Jan. 2008.

[15] L. T. Nguyen, J. Kim, and B. Shim, "Low-rank matrix completion: A contemporary survey," *IEEE Access*, vol. 7, pp. 94215–94237, 2019.

[16] S. L. Brunton, J. H. Tu, I. Bright, and J. N. Kutz, "Compressive sensing and low-rank libraries for classification of bifurcation regimes in nonlinear dynamical systems," *SIAM J. Appl. Dyn. Syst.*, vol. 13, no. 4, pp. 1716–1732, Jan. 2014.

[17] Y.-G. Peng, J.-L. Suo, Q.-H. Dai, and W.-L. Xu, "From compressed sensing to low-rank matrix recovery: Theory and applications," *Acta Automatica Sinica*, vol. 39, no. 7, pp. 981–994, Mar. 2014.

[18] V. Kalofolias, X. Bresson, M. Bronstein, and P. Vandergheynst, "Matrix completion on graphs," 2014, *arXiv:1408.1717*.

[19] M. Zhou, Y. Li, Y. Wang, Q. Pu, X. Yang, and W. Nie, "Device-to-device cooperative positioning via matrix completion and anchor selection," *IEEE Internet Things J.*, vol. 9, no. 7, pp. 5461–5473, Apr. 2022.

[20] X. Guo, L. Chu, and N. Ansari, "Joint localization of multiple sources from incomplete noisy Euclidean distance matrix in wireless networks," *Comput. Commun.*, vol. 122, pp. 20–29, Jun. 2018.

[21] L. T. Nguyen, J. Kim, S. Kim, and B. Shim, "Localization of IoT networks via low-rank matrix completion," *IEEE Trans. Commun.*, vol. 67, no. 8, pp. 5833–5847, Aug. 2019.

[22] R. Du, C. Chen, B. Yang, and X. Guan, "VANET based traffic estimation: A matrix completion approach," in *Proc. IEEE Global Commun. Conf. (GLOBECOM)*, Dec. 2013, pp. 30–35.

[23] R. Du, C. Chen, B. Yang, N. Lu, X. Guan, and X. Shen, "Effective urban traffic monitoring by vehicular sensor networks," *IEEE Trans. Veh. Technol.*, vol. 64, no. 1, pp. 273–286, Jan. 2015.

[24] Z. Kang, C. Peng, and Q. Cheng, "Top-N recommender system via matrix completion," in *Proc. AAAI Conf. Artif. Intell.*, 2016, vol. 30, no. 1, pp. 1–7.

[25] H. Fang, Z. Zhang, Y. Shao, and C.-J. Hsieh, "Improved bounded matrix completion for large-scale recommender systems," in *Proc. IJCAI*, 2017, pp. 1654–1660.

[26] F. Monti, M. M. Bronstein, and X. Bresson, "Deep geometric matrix completion: A new way for recommender systems," in *Proc. IEEE Int. Conf. Acoust., Speech Signal Process. (ICASSP)*, Apr. 2018, pp. 6852–6856.
[27] M. Fazel, "Matrix rank minimization with applications," Ph.D. dissertation, Stanford Univ., Stanford, CA, USA, 2002.
[28] P. Resnick and H. R. Varian, "Recommender systems," *Commun. ACM*, vol. 40, no. 3, pp. 56–58, Mar. 1997.
[29] J. S. Breese, D. Heckerman, and C. kadie, "Empirical analysis of predictive algorithms for collaborative filtering," Microsoft Res. Microsoft Corp. One Microsoft Way, Redmond, WA, USA, Tech. Rep. MSR-TR-98-12, 1998.
[30] E. J. Candes and Y. Plan, "Matrix completion with noise," *Proc. IEEE*, vol. 98, no. 6, pp. 925–936, Jun. 2010.
[31] E. J. Candes and T. Tao, "The power of convex relaxation: Near-optimal matrix completion," *IEEE Trans. Inf. Theory*, vol. 56, no. 5, pp. 2053–2080, May 2010.
[32] J.-F. Cai, E. J. Candès, and Z. Shen, "A singular value thresholding algorithm for matrix completion," *SIAM J. Optim.*, vol. 20, no. 4, pp. 1956–1982, 2010.
[33] X. Peng Li, L. Huang, H. Cheung So, and B. Zhao, "A survey on matrix completion: Perspective of signal processing," 2019, *arXiv:1901.10885*.
[34] K. C. Toh and S. Yun, "An accelerated proximal gradient algorithm for nuclear norm regularized linear least squares problems," *Pacific J. Optim.*, vol. 6, nos. 615–640, p. 15, 2010.
[35] Y. Hu, D. Zhang, J. Ye, X. Li, and X. He, "Fast and accurate matrix completion via truncated nuclear norm regularization," *IEEE Trans. Pattern Anal. Mach. Intell.*, vol. 35, no. 9, pp. 2117–2130, Sep. 2013.
[36] Z. Lin, M. Chen, and Y. Ma, "The augmented Lagrange multiplier method for exact recovery of corrupted low-rank matrices," 2010, *arXiv:1009.5055*.
[37] N. Srebro and R. R. Salakhutdinov, "Collaborative filtering in a non-uniform world: Learning with the weighted trace norm," in *Proc. Adv. Neural Inf. Process. Syst.*, vol. 23, 2010, pp. 1–12.
[38] T. T. Cai and W.-X. Zhou, "Matrix completion via max-norm constrained optimization," *Electron. J. Statist.*, vol. 10, no. 1, Jan. 2016.
[39] E. X. Fang, H. Liu, K.-C. Toh, and W.-X. Zhou, "Max-norm optimization for robust matrix recovery," *Math. Program.*, vol. 167, no. 1, pp. 5–35, Jan. 2018.
[40] X. He, S. Yan, Y. Hu, P. Niyogi, and H.-J. Zhang, "Face recognition using Laplacianfaces," *IEEE Trans. Pattern Anal. Mach. Intell.*, vol. 27, no. 3, pp. 328–340, Mar. 2005.
[41] L. K. Saul and S. T. Roweis, "Think globally, fit locally: Unsupervised learning of low dimensional manifolds," *J. Mach. Learn. Res.*, vol. 4, pp. 119–155, Jun. 2003.
[42] S. P. Chepuri, G. Leus, and A.-J. van der Veen, "Rigid body localization using sensor networks," *IEEE Trans. Signal Process.*, vol. 62, no. 18, pp. 4911–4924, Sep. 2014.
[43] X. Gu, G. Zhou, J. Li, and S. Xie, "Joint time synchronization and ranging for a mobile wireless network," *IEEE Commun. Lett.*, vol. 24, no. 10, pp. 2363–2366, Oct. 2020.
[44] X. Gu, C. Zheng, Z. Li, G. Zhou, H. Zhou, and L. Zhao, "Cooperative localization for UAV systems from the perspective of physical clock synchronization," *IEEE J. Sel. Areas Commun.*, vol. 42, no. 1, pp. 21–33, Jan. 2024.
[45] J. Liu, P. Musialski, P. Wonka, and J. Ye, "Tensor completion for estimating missing values in visual data," *IEEE Trans. Pattern Anal. Mach. Intell.*, vol. 35, no. 1, pp. 208–220, Jan. 2013.
[46] E. Candes and B. Recht, "Exact matrix completion via convex optimization," *Commun. ACM*, vol. 55, no. 6, pp. 111–119, 2012.
[47] S. P. Boyd and L. Vandenberghe, *Convex Optimization*. Cambridge, U.K.: Cambridge Univ. Press, 2004.
[48] M. Grant and S. Boyd. (Mar. 2014). *CVX: MATLAB Software for Disciplined Convex Programming, Version 2.1*. [Online]. Available: http://cvxr.com/cvx
[49] S. R. Becker, E. J. Candès, and M. C. Grant, "Templates for convex cone problems with applications to sparse signal recovery," *Math. Program. Comput.*, vol. 3, no. 3, pp. 165–218, Sep. 2011.
[50] O. Sorkine, "Least-squares rigid motion using SVD," *Computing*, vol. 1, no. 1, pp. 1–5, 2017.
[51] Z.-Q. Luo, W.-K. Ma, A. M.-C. So, Y. Ye, and S. Zhang, "Semidefinite relaxation of quadratic optimization problems," *IEEE Signal Process. Mag.*, vol. 27, no. 3, pp. 20–34, May 2010.

Peiyue Jiang received the B.Eng. degree from Guangdong University of Technology, Guangzhou, China, in 2023. He is currently pursuing the M.Eng. degree with the College of Automation Science and Technology, South China University of Technology. His research interests include signal processing, particularly compressed sensing, cooperative localization, and synchronization.

Xiaobo Gu received the B.Eng. and M.Sc. degrees from the University of Electronic Science and Technology of China, Chengdu, China, in 2008 and 2011, respectively, and the Ph.D. degree from Beihang University, Beijing, China, in 2016. From 2016 to 2018, he was the Director of the Power Dispatching and Control Center, China Southern Power Grid, Guangzhou, China. He is currently an Associate Professor with the School of Integrated Circuits, Guangdong University of Technology, Guangzhou. His research interests include signal processing and communication systems, particularly synchronization, ranging, and positioning techniques for wireless networks.

Haibo Zhou (Senior Member, IEEE) received the Ph.D. degree in information and communication engineering from Shanghai Jiao Tong University, Shanghai, China, in 2014. From 2014 to 2017, he was a Post-Doctoral Fellow with the Broadband Communications Research Group, Department of Electrical and Computer Engineering, University of Waterloo. He is currently a Full Professor with the School of Electronic Science and Engineering, Nanjing University, Nanjing, China. His research interests include resource management and protocol design in B5G/6G networks, vehicular ad hoc networks, and space-air-ground integrated networks. He was a recipient of the 2019 IEEE ComSoc Asia-Pacific Outstanding Young Researcher Award, the 2023–2024 IEEE ComSoc Distinguished Lecturer, and the 2023–2025 IEEE VTS Distinguished Lecturer. He served as the Track Co-Chair/Symposium Co-Chair for IEEE/CIC ICCC 2019, IEEE VTC-Fall 2020, IEEE VTC-Fall 2021, WCSP 2022, IEEE GLOBECOM 2022, and IEEE ICC 2024. He is currently an Associate Editor of IEEE TRANSACTIONS ON WIRELESS COMMUNICATIONS, IEEE INTERNET OF THINGS JOURNAL, *IEEE Network Magazine*, and *Journal of Communications and Information Networks*.